WEP Warwick Evans Publishing

International Journal of Materials Science and Technology Studies

ISSN: 3006-7693 (Print), ISSN: 3006-3744 (Online) | Volume 1, Number 1, Year 2024
DOI: https://doi.org/10.62051//ijmsts.v1n1.09
Journal homepage: https://wepub.org/index.php/IJMSTS/index

Mechanism of interface debonding in steel-concrete components caused by thermal expansion and contraction

Xinkun Niu*

College of Henan Polytechnic University, Jiaozuo, China
*Corresponding Author: Xinkun Niu

ABSTRACT

The steel tube concrete structure constrains the core concrete through the inner wall of the steel tube, forming a hoop effect, significantly improving the compressive performance of the core concrete and effectively exerting the tensile performance of the steel tube. Although this structure has been optimized in terms of mechanical properties, its ultra-high bonding performance makes it extremely difficult to disassemble and recycle. To explore ways to solve this challenge, this article selects C40 concrete as the matrix concrete, and designs and produces circular steel tube concrete specimens and square steel tube concrete specimens with a height of 250mm and a steel tube wall thickness of 4mm. The specific research content covers the hoop effect of steel pipes on core concrete, the degradation law of thermal expansion and contraction interface bonding performance of steel pipe concrete components, the coupling effect of cutting joints and thermal expansion and contraction on interface bonding performance of steel pipe concrete components, and the mechanism of interface debonding of steel pipe concrete components. Through systematic experiments and analysis, the influence of different variation parameters on the debonding performance of steel tube concrete was deeply studied, and its debonding mechanism was revealed. This series of studies provides an important scientific basis for the theoretical understanding and application of steel-concrete structures, helping to overcome the problem of dismantling and recycling, and promoting the transformation and development of related equipment.

KEYWORDS

Steel tube concrete; Hoop effect; Interface bonding performance; Debonding mechanism; Thermal expansion and contraction; Cutting joints

1. INTRODUCTION

Steel tube concrete combines the tensile strength of steel with the compressive strength of concrete, altering the stress performance of concrete and enhancing the stability, load-bearing capacity, and seismic performance of structures. It is widely utilized in large-span structures and high-rise buildings. However, the dismantling and recycling of steel-concrete components still face significant challenges, primarily due to a lack of clear understanding of the debonding mechanism at the steel-concrete interface, thus hindering the provision of theoretical guidance for the renovation or development of specialized dismantling equipment, and consequently industrial dismantling and recycling remain unattainable at present [1-4].

This article focuses on exploring the debonding mechanism of steel tube concrete through systematic research. It conducts a detailed investigation into the influence of the number of shear joints on the debonding performance of the steel tube-concrete interface. The study observes the debonding failure characteristics of the specimen interface under different numbers of shear joints and obtains key

performance indicators such as the load-slip curve and bonding strength. Additionally, the article reveals the theory of normal constraint of steel tubes on core concrete and establishes a mechanical model of the "hoop" effect formed by steel tubes on core concrete. Furthermore, it investigates the influence of thermal expansion and contraction temperature range and the number of cycles on the interfacial debonding performance of square and circular steel tube concrete, and explores the coupling effect between the shear joint and thermal expansion and contraction temperature range. The study observes the debonding failure characteristics of the specimen interface under different variation parameters and obtains key performance indicators such as the load-slip curve and bonding strength of the specimen.

2. EXPERIMENTAL OVERVIEW

The experiment used Q235 seamless steel pipe, and the yield strength, ultimate strength, elastic modulus, and Poisson's ratio of the steel were 328 MPa, 393 MPa, 187 GPa, and 0.273, respectively. The specific measured performance indicators of the steel pipe material are shown in Table 1.

Tabie 1. Mechanical performance indicators of steel

thick[mm]	fy[MPa]	fu[MPa]	E[GPa]	μ
4	328	393	187	0.273

The experiment used P•O 42.5 R grade cement to determine the initial/final setting time, fineness, loss on ignition, compressive strength, and flexural strength of the cement. The results were 183/266 min, 1.29%, 2.38%, 47.2 MPa, and 7.1 MPa, respectively. Natural crushed stone is selected as the coarse aggregate, and its specific physical properties include particle size, apparent density, moisture content, and water absorption. Natural river sand is used as the fine aggregate, and the measured apparent density is 2634 kg/m ³, The bulk density is 1522 kg/m³, The fineness modulus is 2.82, and the specific measured basic physical performance indicators are shown in Table 1;. The water cement ratio and sand ratio of concrete are 0.45 and 37%, respectively. The specific mix proportions of core concrete are shown in Table 2. The mix proportion of concrete in the experiment and the basic mechanical performance test after curing, including the compressive strength of concrete cubes, axial compressive strength, elastic modulus, and splitting tensile strength, are 44.75 MPa, 34.05 MPa, 31.85 GPa, and 2.82 MPa, respectively. The specific mechanical performance indicators of core concrete are shown in Table 3.

Tabie 2. Basic physical properties of coarse aggregate

grain size[mm]	apparent density [kg/m3]	rate of water content [%]	water absorption [%]
5~20	2785	0.5	0.2

Tabie 3. Mixes of concrete

water cement ratio	sand coarse aggregate ratio	Mix water [kg/m3]	cement [kg/m3]	coarse aggregate [kg/m3]	fine aggregate; fines [kg/m3]
0.45	37%	180	400	1140	660

Tabie 4. Mechanical performance index of concrete

fcu [MPa]	fc [MPa]	Ec [GPa]	fst [MPa]
44.75	34.05	31.85	2.82

3. TESTING RESULTS AND ANALYSIS

3.1. Experimental Results And Analysis Of The Hoop Effect Of Steel Pipes On Core Concrete

3.1.1. Experimental phenomena

The failure modes of steel tube concrete under different numbers of cut joints are shown in Figure 1. At the beginning of the experiment, there was no relative slip between the steel pipe and the concrete, but a slight hissing sound could be heard. As the load increases, relative slip develops rapidly, and the sound gradually increases. When approaching the peak load, the specimen emits a crisp "dong dong" sound, with a more stable frequency. The core concrete slides downwards as a whole, causing bonding failure. After unloading, the surface of the concrete at the loading end was slightly broken, and some of the concrete fell off, but it remained as a whole. After the experiment, there is a clear slip joint between the concrete and the steel pipe. The cut joints weaken the constraint of the steel pipe on the concrete, making the specimen more prone to debonding and resulting in a lighter degree of core concrete fragmentation.

(a) C1-25-0 (b) C2-25-0 (c) C3-25-0

Figure 1. The failure modes of specimens

3.1.2. Mechanical model of the "hoop" effect of steel pipes on core concrete

The expansion of the core concrete is caused by cracks, and the hoop effect of the steel pipe will hinder this process, as shown in Figure 2.

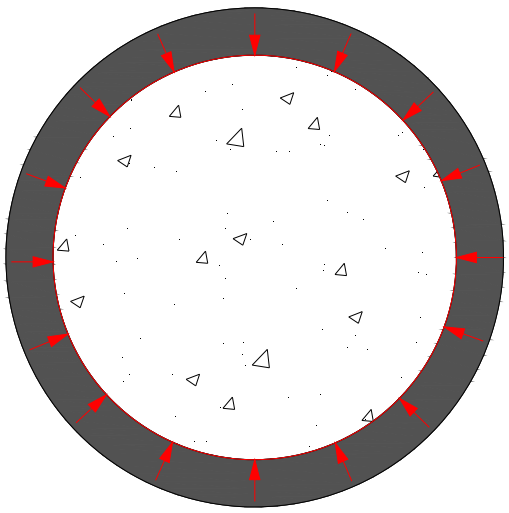

Figure 2. Steel tube constraint on volume expansion of concrete

Conduct a separate analysis of the stress on the core concrete, as shown in Figure 3.

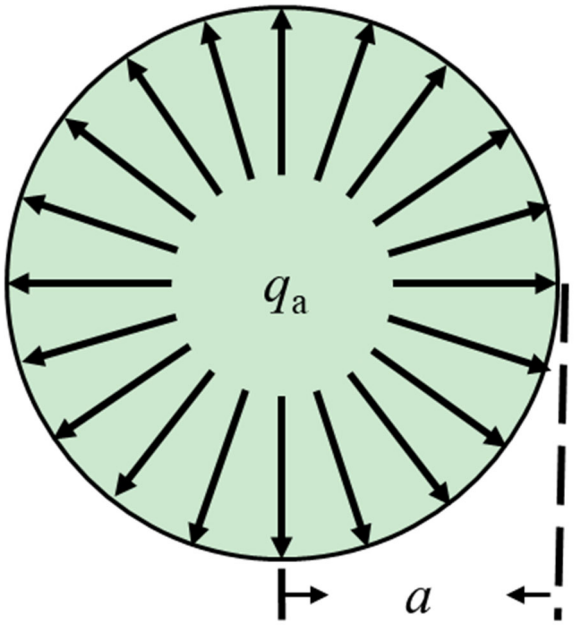

Figure 3. The core concrete is constrained

If the radius of the core concrete is a and the pressure on the steel pipe due to volume expansion is q_a, then the boundary conditions are:

$$(\tau_{\rho\varphi})_{\rho=a} = 0 \tag{1}$$

$$(\tau_{\rho\varphi})_{\rho=b} = 0 \tag{2}$$

$$(\sigma_{\rho})_{\rho=a} = -q_a \tag{3}$$

The stress component is:

$$\sigma_{\rho} = \frac{A}{\rho^2} + B(1+2\ln\rho) + 2C \tag{4}$$

$$\sigma_{\varphi} = -\frac{A}{\rho^2} + B(3+2\ln\rho) + 2C \tag{5}$$

$$\tau_{\rho\varphi} = \tau_{\varphi\rho} = 0 \tag{6}$$

The displacement component under axisymmetric stress state is:

$$u_{\rho} = \frac{1}{E}\left[-(1+\mu)\frac{A}{\rho} + 2(1-\mu)B\rho(\ln\rho - 1) + (1-3\mu)B\rho + 2(1-\mu)C\rho\right] + I\cos\varphi + K\sin\varphi \tag{7}$$

$$u_{\varphi} = \frac{4B\rho\varphi}{E} + H\rho - I\sin\varphi + K\cos\varphi \tag{8}$$

From equations (1), it can be seen that the first two conditions are satisfied, while the latter one is:

$$\frac{A}{a^2}+B(1+2\ln a)+2C=-q_a \tag{9}$$

As can be seen from equation (7), in the expression for circumferential displacement u_φ, $4B\rho\varphi/E$ is an excess value, for the same value ρ, as $\rho=\rho_1$, when $\rho=\rho_1$, and $\varphi=\varphi_1+2\pi$, circumferential displacement difference of $4B\rho\varphi/E$. In a circular ring or cylinder, this is impossible, because ($\rho 1$, $\varphi 1$) and ($\rho_{1,\varphi 1}+2\pi$) are the same point, it is impossible to have different displacements. So according to the displacement single value condition, it is necessary to B=0. In addition, the stress a at the center of the ring should be σ_ρ finite value and must be A=0.

From this, it can be concluded that:

$$2C=-q_a \tag{10a}$$

$$\sigma_\rho=-q_a \tag{10b}$$

From equations (10), it can be seen that the radial pressure in the core concrete is a constant value. Substituting it into the displacement component expression (8), it can be obtained that:

$$u_\rho=\frac{1}{E}\left[-q_a(1-\mu)\rho\right]+I\cos\varphi+K\sin\varphi \tag{11}$$

Among them, I and K are both arbitrary constants, representing the displacement component of the cylinder body.

Due to temperature stress or internal cracks, the core concrete will expand, while the external steel pipe will generate internal pressure on the core concrete due to constraints, causing the core concrete to shrink. The magnitude of shrinkage is linearly related to the internal stress of the steel pipe on the core concrete. Assuming that the chemical bonding force between the steel pipe and the core concrete is τ_a and the dynamic friction coefficient is f_d, the expression for the bonding force between the steel pipe and the core concrete is:

$$\tau=\tau_{\mathrm{a}}+q_a \tag{12}$$

In summary, the larger the volume expansion of the core concrete, the greater the constraint displacement of the steel pipe on the core concrete, and the greater the internal pressure between the steel pipe and the core concrete [6], resulting in an increase in the bonding force between the steel pipe and the core concrete, which is the hoop effect of the steel pipe on the core concrete.

3.2. Research Results And Analysis Of Debonding Test On Thermal Expansion And Contraction Interface Of Steel Tube Concrete

3.2.1. The influence of temperature range of thermal expansion and contraction on bonding performance

(1) Load slip curves of specimens at different temperature ranges under the same number of thermal expansion and contraction cycles:

Under the same number of thermal expansion and contraction cycles, the load displacement curve of square steel tube concrete specimens subjected to high temperatures in different temperature ranges shows a clear evolution process. This curve can be briefly divided into four key stages: straight upward segment, curved upward segment, curved downward segment, and stationary segment.

The initial straight rise section is characterized by the initial load being mainly provided by the chemical bonding force at the interface between the core concrete and the steel pipe. Subsequently, in the curve rise section, the load gradually increases, leading to slight slippage and a decrease in

chemical bonding force, while the mechanical biting force and frictional resistance gradually increase, ultimately causing the specimen to reach its peak load. The appearance of the downward section of the curve indicates that after the specimen reaches the peak load, the slip between the steel pipe and the concrete significantly increases, leading to the complete loss of chemical bonding force. The interfacial bonding force is borne by mechanical biting force and frictional resistance. In the stable stage, the interface friction and wear condition of the specimen tends to stabilize, and the changes in normal stress and frictional resistance are relatively small, causing the bonding stress to gradually stabilize, although relative slip continues to increase.

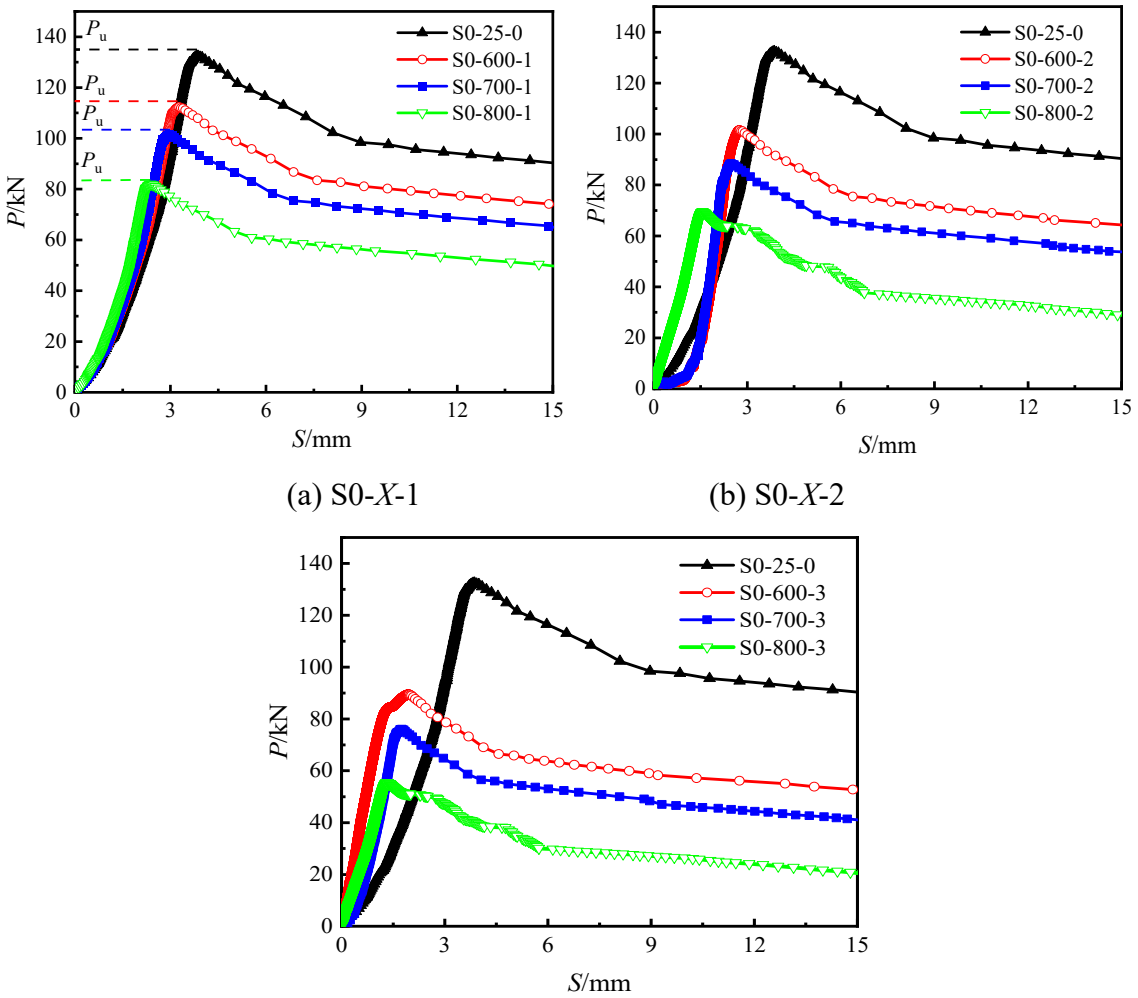

(a) S0-*X*-1 (b) S0-*X*-2

(c) S0-*X*-3

Figure 4. Load displacement curves of square steel tube concrete specimens with different temperature ranges under the same number of thermal expansion and contraction cycles

Under the same number of thermal expansion and cold contraction, the load-displacement curves of concrete specimens with round steel tubes show obvious characteristics after experiencing high temperature in different temperature ranges. Figure 5 shows that with the increase of temperature, the peak load of the specimen gradually decreases, while the peak displacement also decreases.

The high temperature effect causes the concrete structure to become loose, and the evaporation of free water causes the concrete to become looser. During the process of pushing out the load, the interface concrete is more susceptible to shearing, and the thickness of the small concrete particle layer increases, thereby reducing friction resistance and bonding force. Although the core concrete is subjected to expansion deformation caused by the Poisson effect, which generates normal compressive force on the steel pipe wall [7], the change in normal stress caused by the load is

relatively small, the interface wear condition tends to stabilize, the degree of friction resistance change is relatively small, and the interface bonding force tends to stabilize.

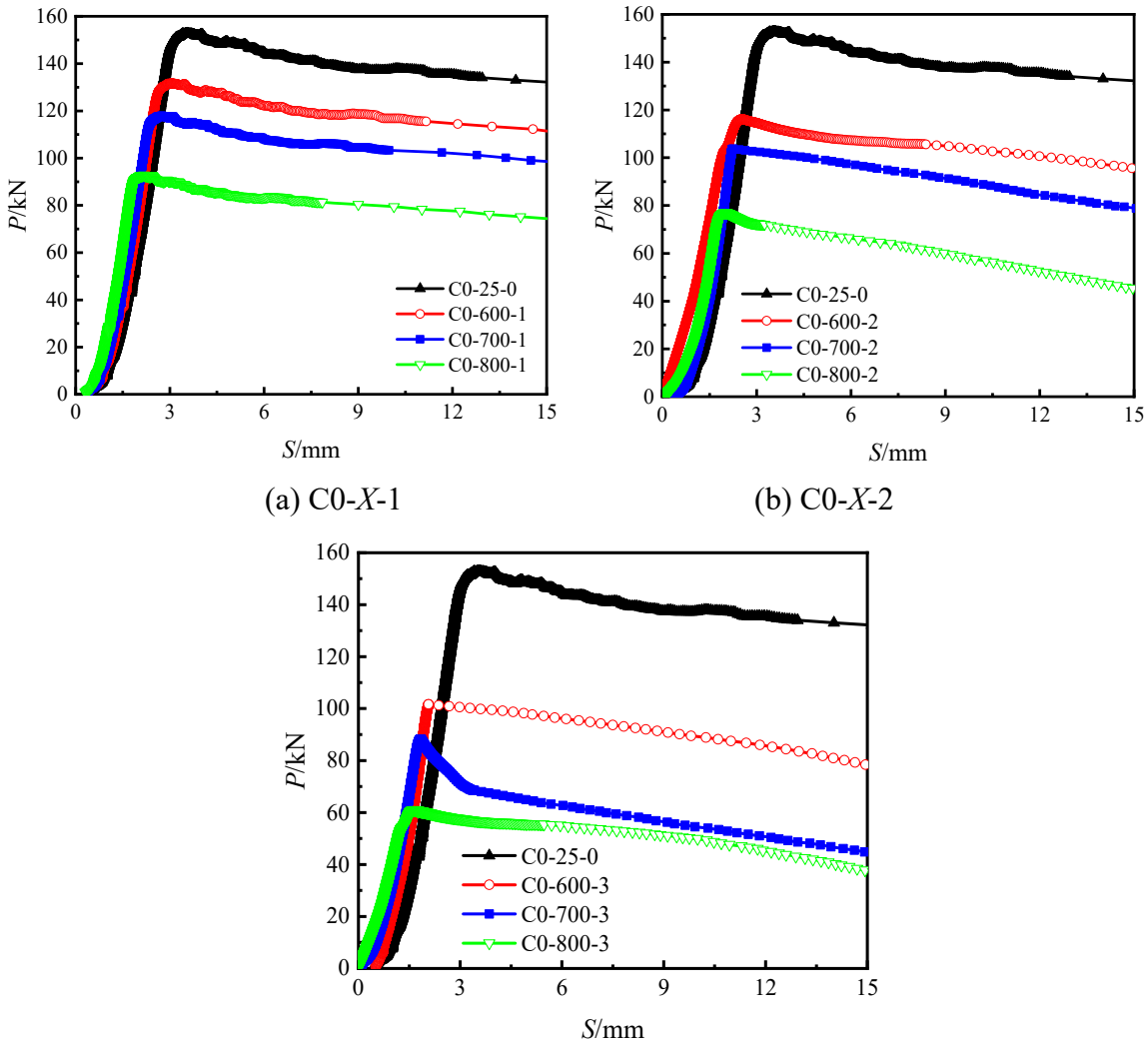

(a) C0-*X*-1 (b) C0-*X*-2

(c) C0-*X*-3

Figure 5. Load displacement curves of circular steel tube concrete specimens with different temperature ranges under the same number of thermal expansion and contraction cycles

(2) Adhesion performance indicators of specimens at different temperature ranges under the same number of thermal expansion and contraction cycles:

Under the same number of thermal expansion and contraction cycles, the bonding performance indicators of square steel tube concrete specimens in different temperature ranges are shown in Table 5, and the variation amplitude of the bonding performance indicators of specimens in different temperature ranges under the same number of thermal expansion and contraction cycles is depicted in Fig 23. It can be observed that as the temperature increases, the bonding strength and bonding stress of the specimen gradually decrease.

When the number of thermal expansion and contraction cycles is one, the bonding forces of the specimen at 600℃, 700℃, and 800℃ are 112.57kN, 101.98kN, and 81.98kN, respectively, and the bonding stresses are 0.63, 0.57, and 0.46. Compared to the C0-25-0 specimen, the bonding force decreased by 15.0%, 23.0%, and 38.1%, respectively.

When the number of thermal expansion and contraction cycles is two, the bonding forces of the specimen at 600℃, 700℃, and 800℃ are 101.58kN, 88.34kN, and 69.40kN, respectively, and the

bonding stresses are 0.57, 0.49, and 0.39. Compared to the C0-25-0 specimen, the bonding force decreased by 23.3%, 33.3%, and 47.6%, respectively.

When the number of thermal expansion and contraction cycles is three, the bonding forces of the specimen at 600℃, 700℃, and 800℃ are 89.40kN, 76.02kN, and 55.36kN, respectively, and the bonding stresses are 0.50, 0.42, and 0.31. Compared to the C0-25-0 specimen, the bonding force decreased by 32.5%, 42.6%, and 58.2%, respectively.

The high temperature effect leads to strength loss of core concrete, severe deterioration of chemical bonding force, dehydration and decomposition of hydration products, and loose concrete structure. Under the action of load, concrete is more prone to breakage, mechanical biting force is reduced, and a layer of small particles is formed at the interface, resulting in reduced frictional resistance. High temperature deteriorates the chemical bonding force, mechanical biting force, and frictional resistance that provide interfacial bonding force, and as the temperature increases, this degradation becomes more pronounced, leading to a decrease in interfacial bonding force. These findings provide important clues for a deeper understanding of the bonding performance of square steel tube concrete under high temperature conditions.

Table 5. Bonding performance indicators of square steel tube concrete specimens in different temperature ranges under the same number of thermal expansion and contraction cycles

Code name	cohesion [kN]	bond stress [MPa]	Relative bonding stress [%]
S0-25-0	132.44	0.74	100
S0-600-1	112.57	0.63	85.0
S0-700-1	101.98	0.57	77.0
S0-800-1	81.98	0.46	61.9
S0-600-2	101.58	0.57	76.7
S0-700-2	88.34	0.49	66.7
S0-800-2	69.40	0.39	52.4
S0-600-3	89.40	0.50	67.5
S0-700-3	76.02	0.42	57.4
S0-800-3	55.36	0.31	41.8

The bonding performance indicators of circular steel tube concrete specimens with different temperature ranges under the same number of thermal expansion and contraction are shown in Table 6. For the convenience of analysis, the variation amplitude of bonding performance indicators of specimens with different temperature ranges under the same number of thermal expansion and contraction is depicted in Figure 24. It can be seen that under the same number of thermal expansion and contraction cycles, as the temperature increases, the bonding strength and bonding stress of the specimen gradually decrease. When the number of thermal expansion and contraction cycles is one, the bonding forces of the specimen at 600℃, 700℃, and 800℃ are 131.50N, 117.82kN, and 92.76kN, respectively. The bonding stresses are 0.84, 0.75, and 0.60, respectively. Compared with the C-25-0 specimen, the bonding forces of the specimen have decreased by 13.9%, 22.9%, and 39.3%, respectively; when the number of thermal expansion and contraction cycles is two, the bonding forces of the specimen at 600℃, 700℃, and 800℃ are 116.14N, 103.76kN, and 77.02kN, respectively. The bonding stresses are 0.74, 0.67, and 0.49, respectively. Compared with the C-25-0 specimen, the bonding forces of the specimen have decreased by 24.0%, 32.1%, and 49.6%, respectively; when the number of thermal expansion and contraction cycles is three, the bonding forces of the specimen at 600℃, 700℃, and 800℃ are 101.62N, 88.17kN, and 60.97kN, respectively. The bonding stresses are 0.65, 0.57, and 0.39, respectively. Compared with the C-25-0 specimen, the bonding forces of the specimen decrease by 33.5%, 42.3%, and 60.1%, respectively. Among them, when the temperature rises to 800℃, the decrease in bonding force is the largest [8]. The reason is that after the specimen

experiences high temperature at 800℃, a large amount of hydration products in the core concrete decompose, causing the concrete mortar matrix to become loose, and high temperature can also cause cracks in the concrete, further reducing the mechanical properties of the core concrete, damaging the chemical bonding force between interfaces [9], and deteriorating the bonding performance to reduce bonding force.

Table 6. Bonding performance indicators of circular steel tube concrete specimens in different temperature ranges under the same number of thermal expansion and contraction cycles

Code name	cohesion (kN)	bond stress (MPa)	Relative bonding stress (%)
C0-25-0	152.81	0.98	100
C0-600-1	131.50	0.84	86.1
C0-700-1	117.82	0.75	77.1
C0-800-1	92.76	0.60	60.7
C0-600-2	116.14	0.74	76.0
C0-700-2	103.76	0.67	67.9
C0-800-2	77.02	0.49	50.4
C0-600-3	101.62	0.65	66.5
C0-700-3	88.17	0.57	57.7
C0-800-3	60.97	0.39	39.9

3.2.3. The influence of thermal expansion and contraction cycles on bonding performance

(1) Load slip curve of specimens with different thermal expansion and contraction cycles at the same temperature:

The load displacement curves of square steel tube concrete specimens with different thermal expansion and contraction cycles at the same temperature are shown in Fig 6. It can be seen that as the number of thermal expansion and contraction cycles increases, the slope of the rising section of the curve gradually increases with the increase of thermal expansion and contraction cycles, and the peak load and peak displacement of the specimen continuously decrease. The reason is that after the specimen experiences high temperature, micro cracks appear in the outer layer of the core concrete due to water evaporation, and the more cycles of thermal expansion and contraction, the more severe the water evaporation of the core concrete, and the more obvious the strength reduction. Additionally, due to the significant difference in thermal performance between concrete and steel pipes, the bonding performance between steel pipes and core concrete is weakened after high temperature. When the specimen cools down after high temperature, shrinkage occurs due to drastic temperature changes. The shrinkage performance of concrete and steel pipes is different, and the bonding force between the interfaces is degraded again. Therefore, as the number of thermal expansion and contraction cycles increases, the damage between the interfaces of the specimen accumulates continuously, the decrease in bonding force increases, and relative slip is more likely to occur during loading. Compared to specimens at room temperature, specimens are more prone to debonding.

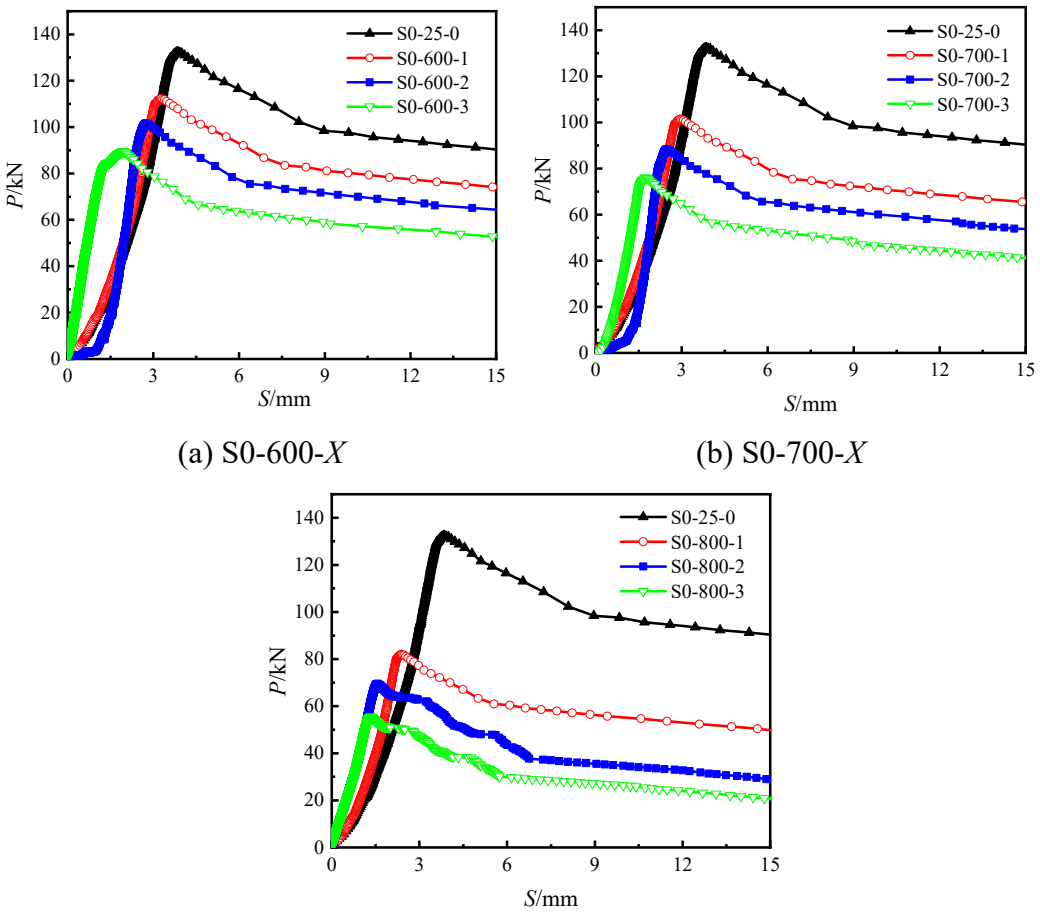

Figure 6. Load displacement curves of square steel tube concrete specimens with different thermal expansion and contraction cycles at the same temperature

The load displacement curves of circular steel tube concrete specimens with different thermal expansion and contraction cycles at the same temperature are shown in Fig 7. It can be seen that as the number of thermal expansion and contraction cycles increases, the peak load of the specimen continuously decreases and the peak displacement continuously decreases. Among them, the load slip curve of the specimen changes most significantly from room temperature to one cycle of thermal expansion and contraction. The reason is that the core concrete of the specimen is tightly connected to the inner wall of the steel pipe at room temperature. After experiencing high temperature, the concrete evaporates free water and the mortar matrix becomes loose. Additionally[10], due to the significant difference in thermal performance between concrete and steel pipe, the concrete expands at high temperature and compresses the steel pipe wall, destroying the chemical bonding force present at the interface, After the heating is completed, when the concrete is taken out from the high-temperature furnace and placed in the ice water mixture, the outer layer of the concrete shrinks due to the severe temperature difference, which deteriorates the bonding force between the interfaces and makes the specimens more prone to debonding. Therefore, in the pushout test loading, compared to specimens at room temperature, specimens that have experienced high temperatures have lower interfacial bonding force and are more likely to experience debonding in advance.

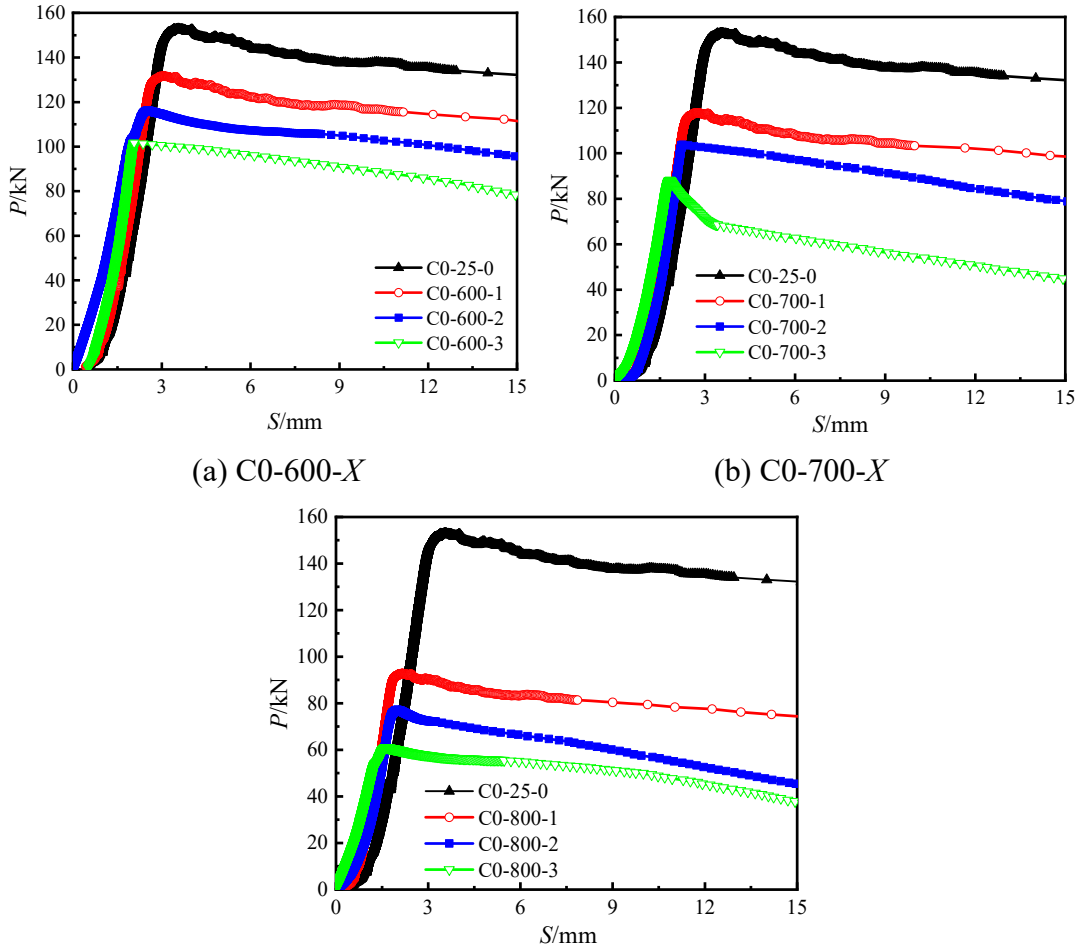

(a) C0-600-*X*

(b) C0-700-*X*

(c) C0-800-*X*

Figure 7. Load displacement curve of circular steel tube concrete specimens with different thermal expansion and contraction cycles at the same temperature

(2) Adhesion performance indicators of specimens with different thermal expansion and contraction cycles at the same temperature:

The bonding performance indicators of square steel tube concrete specimens with different thermal expansion and contraction cycles under the same temperature range are shown in Table 7. For the convenience of analysis, the variation amplitude of the bonding performance indicators of specimens with different thermal expansion and contraction cycles under the same temperature range is depicted in Figure 27. It can be seen that within the same temperature range, as the number of thermal expansion and contraction increases, the bonding strength and bonding stress of the specimen gradually decrease. After experiencing a high temperature of 600℃, the bonding forces of the specimen under the first, second, and third cycles of thermal expansion and contraction were 112.57kN, 101.58kN, and 89.4kN, respectively. The bonding stresses were 0.63, 0.57, and 0.50, respectively. Compared with the C-25-0 specimen, the bonding forces of the specimen decreased by 15%, 23.3%, and 32.5%, respectively; After experiencing a high temperature of 700℃, the bonding forces of the specimen under the first, second, and third cycles of thermal expansion and contraction were 101.98kN, 88.34kN, and 76.02kN, respectively. The bonding stresses were 0.57, 0.49, and 0.42, respectively. Compared with the C-25-0 specimen, the bonding forces of the specimen decreased by 23.0%, 33.3%, and 42.6%, respectively; After experiencing a high temperature of 800℃, the bonding forces of the specimen under the first, second, and third cycles of thermal expansion and contraction were 81.98kN, 69.40kN, and 55.36kN, respectively. The bonding stresses were 0.46, 0.39, and 0.31, respectively. Compared with the C-25-0 specimen, the bonding forces decreased by 38.1%, 47.6%, and 58.2%, respectively. The reason is that the expansion of the core concrete under high temperature

causes temperature cracks, and as the temperature increases, the width and number of cracks also increase. When the specimen is placed in an ice water mixture, the outer surface of the specimen suddenly encounters cold water, causing a sudden temperature drop and a significant difference in temperature between the inside and outside of the steel tube concrete. This temperature causes a huge change in stress gradient, which further leads to the generation and expansion of cracks in the core concrete, The interface bonding force continuously deteriorates, and as the number of thermal expansion and contraction cycles increases, the internal damage of the specimen accumulates, resulting in a continuous decrease in the interface bonding force [11].

Table 7. Bonding performance indicators of square steel tube concrete specimens with different thermal expansion and contraction cycles under the same temperature range

Code name	Cohesion (kN)	bond stress (MPa)	Relative bonding stress (%)
S0-25-0	132.44	0.74	100
S0-600-1	112.57	0.63	85.0
S0-700-1	101.98	0.57	77.0
S0-800-1	81.98	0.46	61.9
S0-600-2	101.58	0.57	76.7
S0-700-2	88.34	0.49	66.7
S0-800-2	69.40	0.39	52.4
S0-600-3	89.40	0.50	67.5
S0-700-3	76.02	0.42	57.4
S0-800-3	55.36	0.31	41.8

The bonding performance indicators of circular steel tube concrete specimens with different thermal expansion and contraction cycles under the same temperature range are shown in Table 8. For the convenience of analysis, the variation amplitude of the bonding performance indicators of specimens with different thermal expansion and contraction cycles under the same temperature range is depicted in Figure 28. It can be seen that within the same temperature range, as the number of thermal expansion and contraction increases, the bonding strength and bonding stress of the specimen gradually decrease. After experiencing a high temperature of 600℃, the bonding forces of the specimen under the first, second, and third cycles of thermal expansion and contraction were 131.50kN, 116.14kN, and 101.62kN, respectively. The bonding stresses were 0.84, 0.74, and 0.65, respectively. Compared with the C-25-0 specimen, the bonding forces of the specimen decreased by 13.9%, 24.0%, and 33.5%, respectively; after experiencing a high temperature of 700℃, the bonding forces of the specimen under the first, second, and third cycles of thermal expansion and contraction were 117.82kN, 103.76kN, and 88.17kN, respectively. The bonding stresses decreased by 22.9%, 32.1%, and 42.3% compared to the C-25-0 specimen, respectively; After experiencing a high temperature of 800℃, the bonding forces of the specimens under the first, second, and third cycles of thermal expansion and contraction were 92.76kN, 77.02kN, and 60.97kN, respectively. The bonding stresses were 0.75, 0.67, and 0.57, respectively. Compared with the C-25-0 specimens, the bonding forces of the specimens decreased by 39.3%, 49.6%, and 60.1%, respectively. Among them, when the specimen undergoes one cycle of thermal expansion and contraction, the interface bonding force and bonding stress of the specimen decrease the most. The reason is that after the specimen experiences high temperature, a large amount of hydration products in the core concrete mortar matrix continuously decompose, free water evaporates, and the concrete volume expands to produce temperature cracks, which deteriorate the connection interface between the steel pipe and concrete. After the high temperature test is completed, when the specimen is placed in the ice water mixture, the outer surface of the specimen suddenly encounters cold water, causing a sudden drop in temperature. There is a significant difference in temperature between the inside and outside of the

steel tube concrete, which is caused by a huge change in stress gradient caused by temperature. This further leads to the generation and expansion of cracks in the core concrete, continuously deteriorating the interfacial bonding force, resulting in a significant decrease in the bonding force and bonding stress of the specimen after one cycle of thermal expansion and contraction. However, as the number of thermal expansion and contraction cycles increases [12], the internal damage of the specimen continues to accumulate, and the interface bonding force is deteriorating more and more seriously. The chemical bonding force between the interfaces is constantly lost, and loose concrete is more easily sheared. Therefore, macroscopically, it is reflected that as the number of thermal expansion and contraction cycles increases, the interface bonding force continuously decreases.

Table 8. Bonding performance indicators of circular steel tube concrete specimens with different thermal expansion and contraction cycles within the same temperature range

Code name	cohesion [kN]	bond stress [MPa]	Relative bonding stress [%]
C0-25-0	152.81	0.98	100
C0-600-1	131.50	0.84	86.1
C0-700-1	117.82	0.75	77.1
C0-800-1	92.76	0.60	60.7
C0-600-2	116.14	0.74	76.0
C0-700-2	103.76	0.67	67.9
C0-800-2	77.02	0.49	50.4
C0-600-3	101.62	0.65	66.5
C0-700-3	88.17	0.57	57.7
C0-800-3	60.97	0.39	39.9

4. CONCLUSIONS

In this paper, the effects of different design parameters on the debonding performance of steel pipe-concrete interface were investigated by launching tests on specimens with different number of cut slits (0, 1, 2), different temperature ranges of thermal expansion and contraction (600℃, 700℃, 800℃), and different number of cycles of thermal expansion and contraction (1, 2, 3 times), and the results showed that:

(1) The destructive process of specimens under different variation parameters is similar, at the end of the test, the upper surface of the concrete at the loading end is slightly broken, and part of the concrete at the interface between the steel pipe and the concrete is dislodged, but the concrete is still a whole unit, and there is an obvious slip joint between the core concrete and the steel pipe. With the increase of the number of slips, the degree of concrete crushing at the interface between the steel pipe and the core concrete gradually decreases. After the specimen experienced high temperature action, the surface color of the core concrete changed from dark gray to light gray, gray-yellow and gray-white, respectively. With the increase of temperature, the broken surface of the core concrete of the round steel pipe concrete specimen is more and more seriously broken, and more concrete fragments are broken along the interface between the steel pipe and the concrete; the corners of the square steel pipe concrete are more seriously damaged.

(2) The load-slip curves of the specimens under different change parameters all show four stages: straight line rising section, curve rising section, curve falling section and smooth section. The specimens with slits have a sudden drop after reaching the peak load, and with the increase of the number of slits, the peak load gradually decreases, and the displacement when reaching the peak load is also gradually smaller. With the increase of the number of slits, the bond strength of the specimens showed a gradual decrease, and the bond strength decreased the most when the number of slits

changed from one slit to two slits, amounting to 47.5%, and the bond strength decreased the least when the number of slits changed from two slits to three slits, amounting to 2.3%. Under the same number of thermal expansion and contraction, with the increase of temperature, the bond strength and bond stress of the specimens showed a gradual decrease. Under the same temperature range, the bond strength and bond stress of the specimens showed a gradual decrease with the increase of the number of thermal expansion and contraction. Under a slit, with the increase of temperature, the bond strength and bond stress of the specimen show a gradual decrease, in which the bond strength of the steel pipe-concrete interface is greatly reduced under the coupling effect of slit and temperature.

(3) Theoretical analysis of the steel pipe normal constraint core concrete, and established the steel pipe on the core concrete "hoop" effect mechanics model, when the core concrete volume expansion is greater, the greater the constraint displacement of the steel pipe on the core concrete, the greater the internal pressure between the steel pipe and the core concrete, the greater the adhesion stress between the steel pipe and the core concrete, the greater the internal pressure between the steel pipe and the core concrete, the greater the internal pressure between the steel pipe and the core concrete, the greater the internal pressure between the steel pipe and the core concrete. The bond stress between steel pipe and core concrete will be increased.

(4) A reasonable finite element model of thermal expansion and contraction of steel pipe and concrete is established by choosing suitable steel and core concrete constitutive relationship and adopting suitable thermal performance parameters of steel and concrete. Under the conditions of constant high temperature and elevated temperature, with the increase of time, the temperature is continuously transferred from the outer surface of the steel pipe to the core concrete, and the isotherm is similar to the shape of the steel pipe cross-section, and the closer to the outer surface of the steel pipe, the larger the temperature gradient is, while the temperature gradient of the core concrete is smaller. Under the condition of constant high temperature, with the increase of time, the temperature stress at the interface of steel pipe and concrete firstly appeared to rise suddenly, then appeared to fall suddenly, and finally tended to stabilize, and under the condition of warming, with the increase of time, the temperature stress at the interface of steel pipe and concrete appeared to increase firstly, then slowly decreased, and finally gradually smoothed out the trend.

REFERENCES

[1] Wu H P, Cui S R, Zhong Z W, et al. Seismic performance test and numerical calculation of shaped multicavitysteel tubular concrete bifurcated short column [J]. Vibration and Shock, 2024, 43(04): 115-124.

[2] Chen M C, Luo S H, Huang H, et al. Experimental study on axial compressive load capacity of locally corroded circular steel pipe concrete short column[J]. Journal of Central South University (Natural Science Edition), 2024, 55(01): 317-329.

[3] Jin L, Liang J, Chen F J, et al. Experimental study on the effect of width-to-thickness ratio on the seismic performance of full-scale square steel pipe concrete short columns [J]. Vibration and Shock, 2023, 42(22): 1-9, 59.

[4] Wang W D, Chen Y M, JI Sunhang, et al. Test and analysis of hysteretic performance of double steel pipe concrete members [J]. Journal of Building Structures, 2024, 45(01): 128-138.

[5] Wang X, Li L, Xiang Y, et al. The influence of basalt fiber on the mechanical performance of concrete-filled steel tube short columns under axial compression [J]. Frontiers in Materials, 2024, 10

[6] Zhang T, Wang Y, Zhai X, et al. Impact response of stainless steel tube locally-strengthened by concrete-filled steel tube [J].International Journal of Impact Engineering, 2024, 186104895-.

[7] Hanqin W, Dianchun X, Qing J, et al. Axial compression performance of concrete-filled-steel tube flat columns with a large steel ratio [J].Structures, 2024, 59105710-.

[8] Sha-Sha S, Ju C, Jun Y, et al. Test and analysis of the interfacial bond behaviour of circular concrete-filled wire-arc additively manufactured steel tubes [J]. Journal of Building Engineering, 2024, 82108171-.

[9] Christo G, S. S S, V. K S, et al. Enhancing the fire-resistant performance of concrete-filled steel tube columns with steel fiber-reinforced concrete [J]. Case Studies in Construction Materials, 2024, 20e02741-.

[10] Dong X, Ye D. A New Method for Correcting the Deviation of a Middle Pier Tower of a Long-Span Intermediate Arch Bridge [J]. Buildings, 2023, 13(10):

[11] Wang L Q, Chu M, Peng K .Analysis on Experimental Performance of Hysteretic Behavior of Concrete-Filled Circular CFRP Steel Tubular Beam-Column [J]. Frontiers in Materials, 2022, 9

[12] Shuaike F, Dongzhi G, Luyao N, et al. Experimental study on seismic behavior of joints connecting precast H-steel reinforced concrete beams and concrete-filled steel tube columns [J]. Journal of Building Engineering, 2022, 45